Polaron features for long-range electron–phonon interaction

2004 J. Phys.: Condens. Matter 16 1593

(http://iopscience.iop.org/0953-8984/16/9/007)

INSTITUTE OF PHYSICS PUBLISHING JOURNAL OF PHYSICS: CONDENSED MATTER

J. Phys.: Condens. Matter **16** (2004) 1593–1601 PII: S0953-8984(04)73245-2

Polaron features for long-range electron–phonon interaction

C A Perroni, V Cataudella and G De Filippis

Coherentia-INFM and Dipartimento di Scienze Fisiche, Università degli Studi di Napoli 'Federico II', Complesso Universitario Monte Sant'Angelo, Via Cintia, I-80126 Napoli, Italy

Received 10 December 2003
Published 20 February 2004
Online at stacks.iop.org/JPhysCM/16/1593 (DOI: 10.1088/0953-8984/16/9/007)

Abstract

The polaron features for long-range electron–phonon interaction are investigated by extending a variational approach previously proposed for the study of systems with local coupling. The ground state spectral weight, the average kinetic energy, the mean number of phonons, and the electron–lattice correlation function are discussed for a wide range of model parameters focusing on the adiabatic regime and comparing the results with the short-range case (Holstein model). A strong mixing of electronic and phononic degrees of freedom for small values of the electron–phonon coupling constant is found in the adiabatic case due to the long-range interaction. Finally a polaron 'phase diagram' is proposed.

1. Introduction

In recent years many experimental results have pointed out the presence of strong electron–phonon (el–ph) coupling and polaronic effects in several compounds, such as high-temperature cuprate superconductors and colossal magnetoresistance manganites [1, 2]. This large amount of experimental data has renewed the interest in studying simplified el–ph coupled systems of the Holstein [3] or Fröhlich [4] type and in proposing more realistic interaction models [5, 6].

The Holstein molecular crystal model is the prototype for short-range (SR) el–ph interaction since it takes into account local coupling of a tight-binding electron to optical local phonon modes. Until now an exact solution for this model has not been found, and perturbative expansions are not able to describe the most interesting region characterized by intermediate el–ph couplings and electron and phonon energy scales are not well separated. In this regime, as shown by several numerical studies [7–11] and variational approaches [12–14], the system undergoes a crossover from a weakly dressed electron to a massive localized polaronic quasiparticle, the small Holstein polaron (SHP), with increasing the strength of interaction. All the ground state properties of the Holstein model can be described with great accuracy by a variational approach [13, 14] based on a linear superposition of Bloch states that describe weak and strong coupling polaron wavefunctions. Indeed this method provides

an immediate physical interpretation of the intermediate regime and is in excellent agreement with numerical results.

Recently a quite general el–ph lattice Hamiltonian with a 'density-displacement' type interaction has been introduced in order to understand the role of long-range (LR) coupling on the polaron formation [5, 15]. The model for a single particle is described by the Hamiltonian H:

$$H = -t \sum_{\langle i,j \rangle} c_i^\dagger c_j + \omega_0 \sum_i \left(a_i^\dagger a_i + \tfrac{1}{2}\right) + \alpha\omega_0 \sum_{i,j} f(|\vec{R}_i - \vec{R}_j|) c_i^\dagger c_i \left(a_j + a_j^\dagger\right). \tag{1}$$

The units are such that $\hbar = 1$. In equation (1) $c_i^\dagger (c_i)$ denotes the electron creation (annihilation) operator at site i, whose position vector is indicated by $\vec{R}_i$, and the symbol $\langle\,\rangle$ denotes nearest neighbours linked through the transfer integral t. The operator $a_i^\dagger (a_i)$ represents the creation (annihilation) operator for a phonon on the site i, ω_0 is the frequency of the optical local phonon modes, α controls the strength of el–ph coupling, and $f(|\vec{R}_i - \vec{R}_j|)$ is the interacting force between an electron on the site i and an ion displacement on the site j.

The Hamiltonian (1) reduces to the Holstein model if $f(|\vec{R}_i - \vec{R}_j|) = \delta_{\vec{R}_i,\vec{R}_j}$, while in general it contains LR interaction. In particular when one attempts to mimic the nonscreened coupling between doped holes and apical oxygen in some cuprates [5], the interaction force is given by

$$f(|\vec{R}_i - \vec{R}_j|) = (|\vec{R}_i - \vec{R}_j|^2 + 1)^{-\frac{3}{2}}, \tag{2}$$

if the distance $|\vec{R}_i - \vec{R}_j|$ is measured in units of lattice constant. Considering the general el–ph matrix element $M_{\vec{q}}$

$$M_{\vec{q}} = \frac{\alpha\omega_0}{\sqrt{L}} \sum_m f(|\vec{R}_m|) \mathrm{e}^{\mathrm{i}\vec{q}\cdot\vec{R}_m}, \tag{3}$$

with L number of lattice sites, we can define the polaronic shift E_p

$$E_\mathrm{p} = \sum_{\vec{q}} \frac{M_{\vec{q}}^2}{\omega_0}, \tag{4}$$

and the coupling constant $\lambda = E_\mathrm{p}/zt$, with z lattice coordination number, that represents a natural measure of the strength of the el–ph interaction in both the SR and LR case. Clearly for LR interaction forces the matrix element $M_{\vec{q}}$ is peaked around $\vec{q} = 0$. Since it has been claimed that the enhancement of the forward direction in the el–ph scattering could play a role in explaining several anomalous properties of cuprates such as the linear temperature behaviour of the resistivity and the d-wave symmetry of the superconducting gap [16, 17], the study of lattice polaron features for LR interactions is important in order to clarify the role of the el–ph coupling in complex systems.

When the interaction force is given by equation (2), the model has been investigated applying a path-integral Monte Carlo (PIMC) algorithm [5, 15] efficient in the thermodynamic limit. The first investigations have been mainly limited to the determination of the polaron effective mass pointing out that, due to the LR coupling, the polaron is much lighter than the SHP with the same binding energy in the strong coupling regime. Furthermore it has been found that this effect due to the weaker band renormalization becomes smaller in the antiadiabatic regime. Then the quasiparticle properties have been studied by an exact Lanczos diagonalization method [18] on finite one-dimensional lattices (up to 10 sites) making a close comparison with the corresponding properties of HP. As a result of the LR interaction, the lattice deformation induced by the electron is spread over many lattice sites in the strong coupling region, giving rise to the formation of a large polaron (LP) as in the weak coupling

regime. All numerical and analytical results have been mainly obtained in the antiadiabatic and nonadiabatic regime. Only recently has the behaviour of the effective mass of a two-site system [19] in the adiabatic regime been studied within the nearest-neighbour approximation for the el–ph interaction confirming that the LP is lighter than the SHP at strong coupling.

In this paper we pursue the study of the ground state of the model with the interaction force given by equation (2) in the thermodynamic limit. We employ a variational approach previously proposed for the study of systems with el–ph local coupling [13, 14] and based on a linear superposition of Bloch states that describe weak and strong coupling polaron wavefunctions. Although the method is valid for any spatial dimension, we limit our study to the one-dimensional case. It has been found that the variational approach provides an estimate of the ground state energy in good agreement with PIMC results. The evolution of the ground state spectral weight, the average kinetic energy, the mean number of phonons, and the electron–lattice correlation function with respect to the adiabaticity ratio ω_0/t and the el–ph coupling constant is discussed, focusing on the adiabatic regime. Indeed, in the adiabatic case, there is a range of values of the el–ph coupling where the ground state is well described by a particle with a weakly renormalized mass but a spectral weight much smaller than unity. Furthermore, with increasing the strength of interaction in the same regime, the renormalized mass gradually increases, while the average kinetic energy is not strongly reduced. Finally, regions of the model parameters are distinguished according to the values assumed by the spectral weight. The resulting 'phase diagram'[1] shows strong mixing of electronic and phononic degrees of freedom for small values of the el–ph coupling constant in the adiabatic case.

2. Variational wavefunction

The variational approach is summarized following the lines of previous works [13, 14].

We consider as trial wavefunctions translational invariant Bloch states obtained by taking a superposition of localized states centered on different lattice sites:

$$|\psi_{\vec{k}}^{(i)}\rangle = \frac{1}{\sqrt{L}} \sum_{\vec{R}_n} \mathrm{e}^{\mathrm{i}\vec{k}\cdot\vec{R}_n} |\psi_{\vec{k}}^{(i)}(\vec{R}_n)\rangle, \tag{5}$$

where

$$|\psi_{\vec{k}}^{(i)}(\vec{R}_n)\rangle = \exp\left(\sum_{\vec{q}} \left[h_{\vec{q}}^{(i)}(\vec{k}) a_{\vec{q}} \mathrm{e}^{\mathrm{i}\vec{q}\cdot\vec{R}_n} + \mathrm{h.c.} \right] \right) \sum_m \phi_{\vec{k}}^{(i)}(\vec{R}_m) c_{m+n}^{\dagger} |0\rangle. \tag{6}$$

In equation (5) the apex $i = w, s$ indicates the weak and strong coupling polaron wavefunction, respectively, $|0\rangle$ denotes the electron and phonon vacuum state, and $\phi_{\vec{k}}^{(i)}(\vec{R}_m)$ are variational parameters defining the spatial broadening of the electronic wavefunction. The phonon distribution functions $h_{\vec{q}}^{(i)}(\vec{k})$ are chosen in order to reproduce the description of polaron features in the two asymptotic limits [13]. Therefore the weak coupling phonon distribution function $h_{\vec{q}}^{(\mathrm{w})}(\vec{k})$ is assumed as

$$h_{\vec{q}}^{(\mathrm{w})}(\vec{k}) = \frac{M_{\vec{q}}}{\omega_0 + E_{\mathrm{b}}(\vec{k}+\vec{q}) - E_{\mathrm{b}}(\vec{k})}, \tag{7}$$

where $E_{\mathrm{b}}(\vec{k})$ is the free electron band energy, while the strong coupling phonon distribution function $h_{\vec{q}}^{(\mathrm{s})}(\vec{k})$ is

$$h_{\vec{q}}^{(\mathrm{s})}(\vec{k}) = \frac{M_{\vec{q}}}{\omega_0} \sum_m |\phi_{\vec{k}}(\vec{R}_m)|^2 \mathrm{e}^{\mathrm{i}\vec{q}\cdot\vec{R}_m}. \tag{8}$$

[1] We use the phrase phase diagram between inverted commas to indicate that there is no true phase transition in this one-electron system but a crossover from a quasi-free electron to a carrier strongly coupled to the lattice.

A careful inspection of weak and strong coupling wavefunctions shows that in the intermediate regime they are not orthogonal and the off-diagonal matrix elements of the Hamiltonian are not zero. Hence the ground state energy is determined by considering as trial state a linear superposition of the weak and strong coupling wavefunctions:

$$|\psi_{\vec{k}}\rangle = \frac{A_{\vec{k}}|\overline{\psi}_{\vec{k}}^{(\mathrm{w})}\rangle + B_{\vec{k}}|\overline{\psi}_{\vec{k}}^{(\mathrm{s})}\rangle}{\sqrt{A_{\vec{k}}^2 + B_{\vec{k}}^2 + 2A_{\vec{k}}B_{\vec{k}}S_{\vec{k}}}}, \tag{9}$$

where

$$|\overline{\psi}_{\vec{k}}^{(\mathrm{w})}\rangle = \frac{|\psi_{\vec{k}}^{(\mathrm{w})}\rangle}{\sqrt{\langle\psi_{\vec{k}}^{(\mathrm{w})}|\psi_{\vec{k}}^{(\mathrm{w})}\rangle}}, \qquad |\overline{\psi}_{\vec{k}}^{(\mathrm{s})}\rangle = \frac{|\psi_{\vec{k}}^{(\mathrm{s})}\rangle}{\sqrt{\langle\psi_{\vec{k}}^{(\mathrm{s})}|\psi_{\vec{k}}^{(\mathrm{s})}\rangle}} \tag{10}$$

and $S_{\vec{k}}$

$$S_{\vec{k}} = \frac{\langle\overline{\psi}_{\vec{k}}^{(\mathrm{w})}|\overline{\psi}_{\vec{k}}^{(\mathrm{s})}\rangle + \mathrm{h.c.}}{2} \tag{11}$$

is the overlap factor of the two wavefunctions $|\overline{\psi}_{\vec{k}}^{(\mathrm{w})}\rangle$ and $|\overline{\psi}_{\vec{k}}^{(\mathrm{s})}\rangle$. In equation (9), $A_{\vec{k}}$ and $B_{\vec{k}}$ are two additional variational parameters which provide the relative weight of the weak and strong coupling solutions of the system for any particular value of $\vec{k}$.

We perform the minimization procedure with respect to the parameters $\phi_{\vec{k}}^{(\mathrm{w})}(\vec{R}_m)$, $\phi_{\vec{k}}^{(\mathrm{s})}(\vec{R}_m)$, $A_{\vec{k}}$ and $B_{\vec{k}}$, assuming

$$\phi_{\vec{k}}^{(i)}(\vec{R}_n) = \alpha_{\vec{k}}^{(i)}\delta_{\vec{R}_n,0} + \beta_{\vec{k}}^{(i)}\sum_{\delta}\delta_{\vec{R}_n,\vec{\delta}} + \gamma_{\vec{k}}^{(i)}\sum_{\delta'}\delta_{\vec{R}_n,\vec{\delta}'} + \eta_{\vec{k}}^{(i)}\sum_{\delta''}\delta_{\vec{R}_n,\vec{\delta}''}, \tag{12}$$

where the quantities $\alpha_{\vec{k}}^{(i)}$, $\beta_{\vec{k}}^{(i)}$, $\gamma_{\vec{k}}^{(i)}$, and $\eta_{\vec{k}}^{(i)}$ denote variational parameters, and the symbols δ, δ', δ'' indicate, respectively, the nearest, the next-nearest neighbours and so on. This choice takes into account the broadening of the electron wavefunctions up to third neighbours and provides an accurate description of the polaron features for any value of the parameters of the Hamiltonian. The ground state energies obtained with this choice are slightly higher than PIMC mean energies, the difference being less than 0.5% in the worst case of intermediate regime. We note that these wavefunctions can be improved by adding further terms in equation (12), so it is possible to obtain better and better estimates of the energy.

3. Results

In this paper we study the properties of the ground state in the one-dimensional case.

In figure 1(a) we report the polaron ground state energy for different values of the adiabaticity ratio as a function of the el–ph constant coupling α. We have checked that our variational proposal recovers the asymptotic perturbative results and significantly improves these asymptotic estimates in the intermediate region. Moreover, our data for the ground state energy in the intermediate region are in very good agreement with the results of the PIMC approach [5] shown as diamonds in figure 1(a). The consistency of the results with a numerically more sophisticated approach indicates that the true wavefunction is very close to a superposition of weak and strong coupling states.

Another property of interest is the ground state spectral weight Z,

$$Z = Z_{k=0} = |\langle\psi_{k=0}|c_{k=0}^{\dagger}|0\rangle|^2, \tag{13}$$

that gives the fraction of the bare electron state in the polaronic trial wavefunction. It measures how much the quasiparticle is different from the free electron ($Z = 1$), and a small value

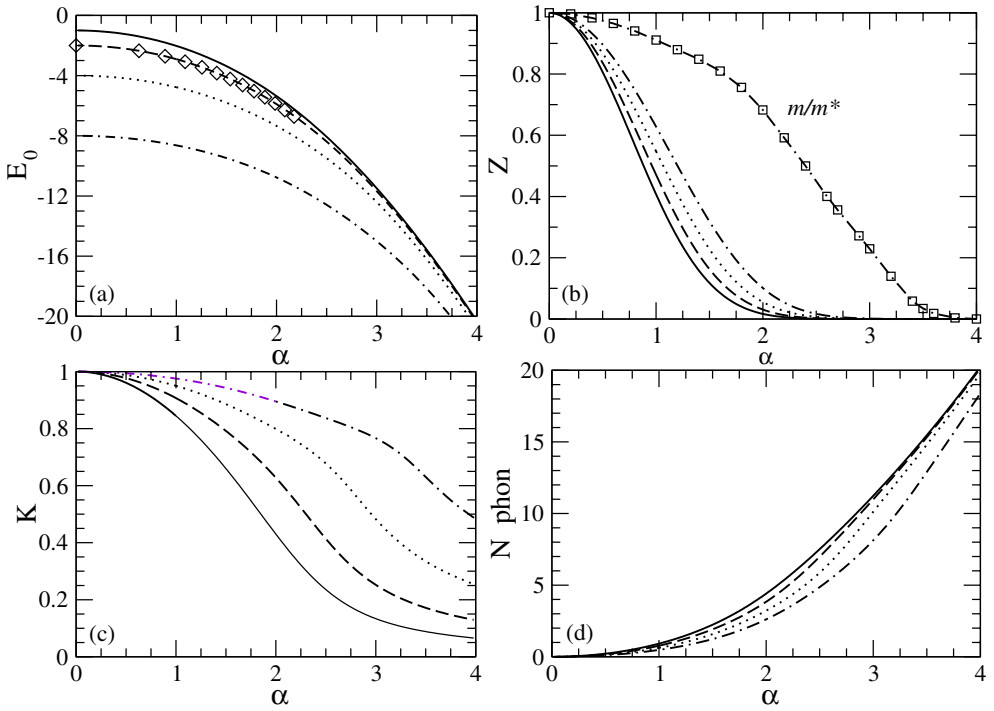

Figure 1. The ground state energy E_0 in units of ω_0 (a), the spectral weight Z (b), the average kinetic energy K (c) and the average phonon number N (d) as a function of the coupling constant α for different values of the adiabatic ratio: $\omega_0/t = 2$ (solid curve), $\omega_0/t = 1$ (dashed curve), $\omega_0/t = 0.5$ (dotted line) and $\omega_0/t = 0.25$ (dash–dotted curve). The diamonds in (a) indicate the PIMC data for the energy kindly provided by Kornilovitch at $\omega_0/t = 1$, and the squares on a dash–dotted curve in (b) denote the ratio m/m^* obtained within the variational approach at $\omega_0/t = 0.25$.

of Z indicates a strong mixing of electronic and phononic degrees of freedom. As plotted in figure 1(b), the increase of the el–ph coupling strength induces a decrease of the spectral weight that is smooth also in the adiabatic regime. The reduction of Z is closely related to the decrease of the Drude weight obtained by exact diagonalizations [18] pointing out a gradual suppression of coherent motion. We note that the behaviour of Z is different from that of the local Holstein model. In fact for the latter, Z results in being very close to the ratio m/m^*, with m and m^* the bare electron and effective polaron mass, respectively [18], while for LR couplings $Z < m/m^*$ in the intermediate to strong coupling adiabatic regime. This relation is confirmed by the results shown in figure 1(b), where the dash–dotted curve and the squares on a similar line indicate the spectral weight Z and the ratio m/m^* obtained within the variational approach, respectively, as a function of the coupling constant α at $\omega_0/t = 0.25$ [15]. Actually there is a large region of the parameters in the adiabatic regime where the ground state is well described by a particle with a weakly renormalized mass but a spectral weight Z much smaller than unity. While the electron drags the phonon cloud coherently through the lattice, with increasing the el–ph coupling in the adiabatic case, a band collapse occurs in the SR case, while the particle undergoes a weaker band renormalization in the case of LR interactions. Therefore in the LR case the polaron results in being lighter than the SHP in the intermediate to strong coupling adiabatic regime.

Insight about the electron state is obtained by calculating its kinetic energy K in units of the bare one. Since the average kinetic energy gives the total weight of the optical conductivity,

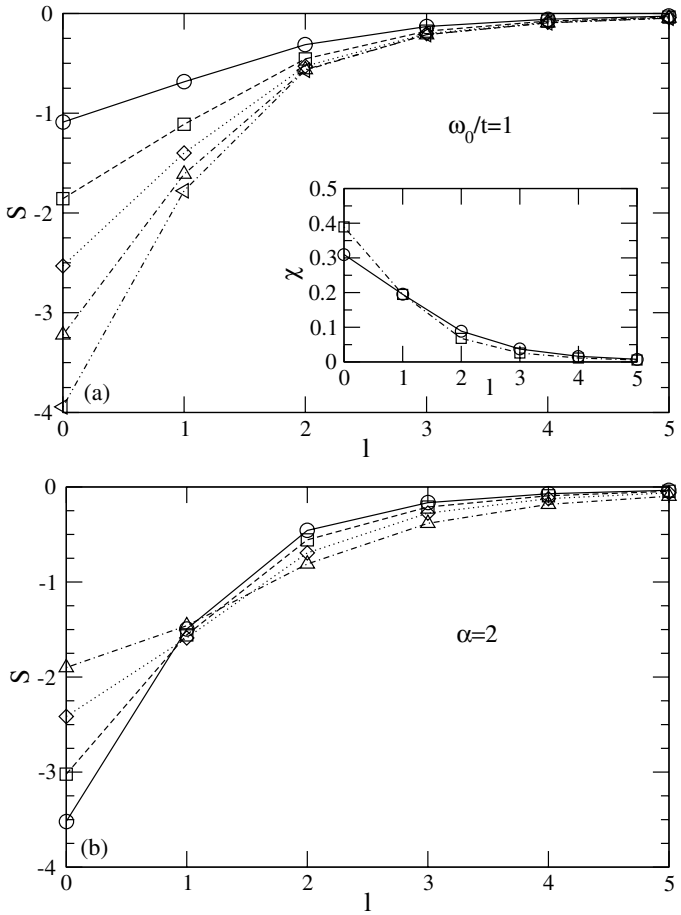

Figure 2. (a) The electron–lattice correlation function $S(R_l)$ at $\omega_0/t = 1$ for different values of the coupling: $\lambda = 0.5$ (circles), $\lambda = 1.25$ (squares), $\lambda = 2.0$ (diamonds), $\lambda = 2.75$ (triangles up), and $\lambda = 3.5$ (triangles down). In the inset the normalized correlation function $\chi(R_l)$ at $\omega_0/t = 1$ is shown for $\lambda = 0.5$ (circles) and $\lambda = 2.75$ (squares). (b) The electron–lattice correlation function $S(R_l)$ at $\alpha = 2$ for different values of the adiabatic parameter: $\omega_0/t = 2$ (circles), $\omega_0/t = 1$ (squares), $\omega_0/t = 0.5$ (diamonds), and $\omega_0/t = 0.25$ (triangles up).

K includes both coherent and incoherent transport processes [18]. As reported in figures 1(b) and (c), in the strong coupling adiabatic region before the electron is selftrapped ($K \ll 1$), the average kinetic energy is weakly renormalized, the ratio m/m^* is reduced and the spectral weight is nearly zero. Furthermore, in figures 1(c) and (d), within the adiabatic regime, the average kinetic energy and the mean number of phonons do not show any sharp change by increasing the el–ph coupling.

Another quantity associated with polaron formation is the correlation function $S(R_l)$,

$$S(R_l) = S_{k=0}(R_l) = \frac{\sum_n \langle \psi_{k=0} | c_n^\dagger c_n \left(a_{n+l}^\dagger + a_{n+l} \right) | \psi_{k=0} \rangle}{\langle \psi_{k=0} | \psi_{k=0} \rangle}, \tag{14}$$

or equivalently the normalized correlation function $\chi(R_l) = S(R_l)/N$, with $N = \sum_l S(R_l)$. In figure 2(a) we report the correlation function $S(R_l)$ at $\omega_0/t = 1$ for several values of the el–ph interaction. The lattice deformation is spread over many lattice sites giving rise to the formation

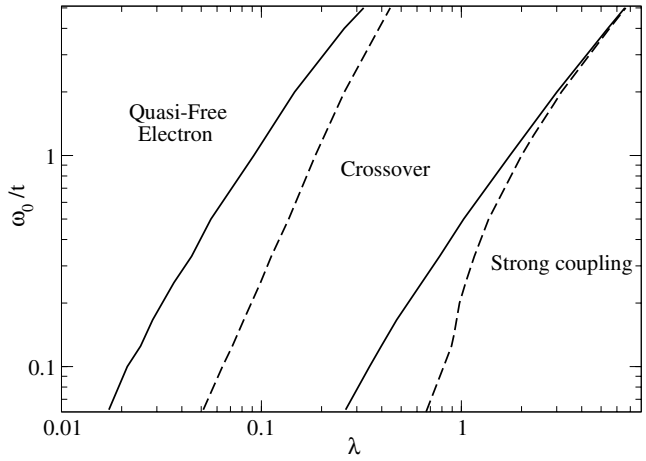

Figure 3. Polaron 'phase diagram' for long-range (solid curve) and Holstein (dashed curve) el–ph interaction. The transition lines correspond in weak coupling to model parameters such that the spectral weight $Z = 0.9$, in strong coupling such that $Z = 0.1$.

of LP also in the strong coupling regime where really the correlation function assumes the largest values. In the inset of figure 2(a) the normalized electron–lattice correlation function χ shows consistency with the corresponding quantity calculated in a previous work [18]. While in the weak coupling regime the amplitude χ is smaller than the quantum lattice fluctuations, increasing the strength of the interaction, it becomes stronger and the lattice deformation is able to generate an attractive potential that can trap the charge carrier. Clearly, even if the correlations between electron and lattice are large, the resulting polaron is delocalized over the lattice due to the translational invariance. Finally, the variation of the lattice deformation as a function of ω_0/t shown in figure 2(b) can be understood as a retardation effect. In fact, for small ω_0/t, the less numerous phonons excited by the passage of the electron take a long time to relax; therefore the lattice deformation increases far away from the current position of the electron.

In figure 3 we propose a 'phase diagram' based on the values assumed by the spectral weight in analogy with the Holstein polaron [14]. Analysing the behaviour of Z it is possible to distinguish three different regimes:

(1) quasi-free-electron regime ($0.9 < Z < 1$) where the electron has a weakly renormalized mass and the motion is coherent;
(2) crossover regime ($0.1 < Z < 0.9$) characterized by intermediate values of spectral weight and a mass not strongly enhanced;
(3) strong coupling regime ($Z < 0.1$) where the spectral weight is negligible and the mass is large but not enormous.

We note that for LR interactions in the adiabatic case there is strong mixing of electronic and phononic degrees of freedom for values of the coupling constant λ (solid curves) smaller than those characteristic of local Holstein interaction (dashed curves). Furthermore, in this case, entering the strong coupling regime, the charge carrier does not undergo any abrupt localization; on the contrary, as indicated also by the behaviour of the average kinetic energy K, it is quite mobile.

In order to study the effects of different el–ph interactions, we have evaluated the average kinetic energy for both LR and SR cases. As reported in figure 4(a), in excellent agreement

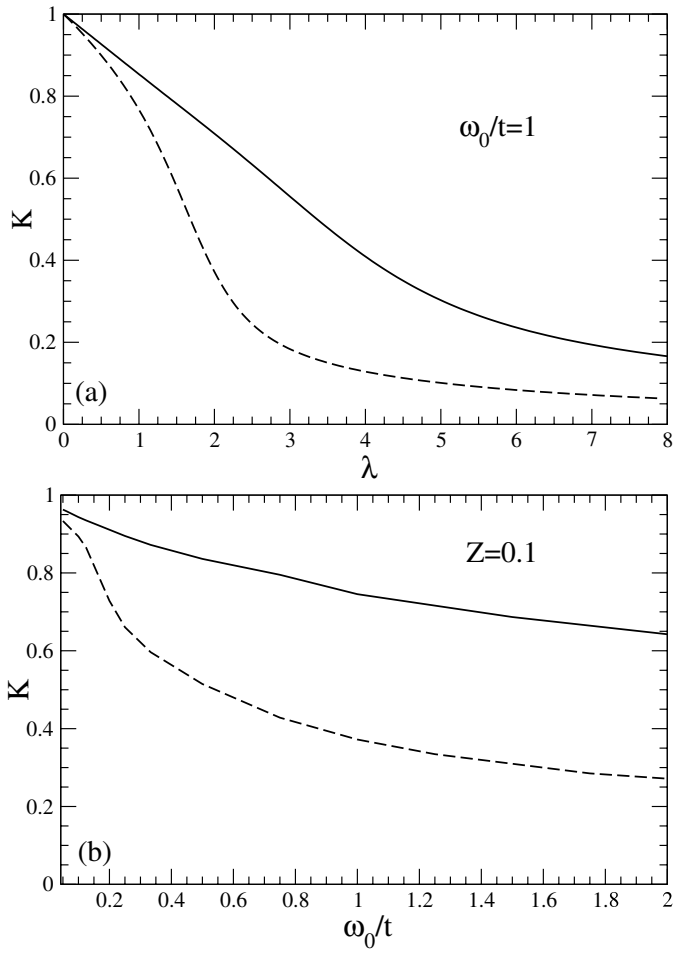

Figure 4. (a) The average kinetic energy K as a function of the constant coupling λ at $\omega_0/t = 1$ for long-range (solid curve) and local Holstein el–ph interaction (dashed curve). (b) The average kinetic energy K as a function of the adiabaticity ratio ω_0/t for long-range (solid curve) and Holstein (dashed curve) el–ph interaction in correspondence of model parameters such that the spectral weight $Z = 0.1$.

with a previous study [18], for LR interactions K decreases very gradually with increasing λ. Furthermore, if the regime of parameters where the spectral weight $Z = 0.1$ is considered, as shown in figure 4(b), in the adiabatic case the average kinetic energy is larger for LR interactions (solid curve) with respect to local Holstein ones (dashed curve). The comparison emphasizes that due to LR interactions in the adiabatic regime K is slightly renormalized even if the coherent motion is small.

4. Conclusions

In this paper we have extended a previous variational approach in order to study the polaronic ground state features of a one-dimensional el–ph model with long-range interaction. The trial function is based on a linear superposition of Bloch states that describe weak and strong

coupling polaron wavefunctions and it provides an estimate of the ground state energy in good agreement with numerical methods. The results relative to spectral weight, the average kinetic energy, the mean number of phonons, and the electron–lattice correlation function have been discussed mainly in the adiabatic regime. It has been possible to identify a range of intermediate values of the el–ph coupling constant in the adiabatic case where the system is well described by a particle characterized with a weakly renormalized mass but a small spectral weight. In the same regime, further increasing the el–ph coupling, the renormalized mass shows a smooth increase, while the average kinetic energy is not strongly reduced. Finally we have proposed a 'phase diagram' according to the values assumed by the spectral weight. It is found that there is strong mixing between electronic and phononic degrees of freedom for small values of the el–ph coupling constant in the adiabatic case.

The variational approach can be easily generalized to high dimensions [13], and it has been recently applied to study the three-dimensional continuum Fröhlich model, giving a very good description of ground state features [20]. In any case the results discussed in this paper are not limited to the one-dimensional case as confirmed by the behaviour of some properties on the square lattice [5, 15].

References

[1] Zhao G-M, Hunt M B, Keller H and Muller K A 1997 *Nature* **385** 236
Lanzara A, Bogdanov P V, Zhou X J, Kellar S A, Feng D L, Lu E D, Yoshida T, Eisaki H, Fujimori A, Kishio K, Shimoyama J-I, Noda T, Uchida S, Hussain Z and Shen Z-X 2001 *Nature* **412** 510
McQueeney R J, Sarrao J L, Pagliuso P G, Stephens P W and Osborn R 2001 *Phys. Rev. Lett.* **87** 77001

[2] De Teresa J M, Ibarra M R, Algarabel P A, Ritter C, Marquina C, Blasco J, Garcia J, del Moral A and Arnold Z 1997 *Nature* **386** 256
Millis A J 1998 *Nature* **392** 147
Salamon M B and Jaime M 2001 *Rev. Mod. Phys.* **73** 583

[3] Holstein T 1959 *Ann. Phys., Lpz.* **8** 325
Holstein T 1959 *Ann. Phys., Lpz.* **8** 343

[4] Fröhlich H 1954 *Adv. Phys.* **3** 325

[5] Alexandrov A S and Kornilovitch P E 1999 *Phys. Rev. Lett.* **82** 807

[6] Sandvik A W, Scalapino D J and Bickers N E 2003 *Preprint* cond-mat/0309171

[7] de Raedt H and Lagendijk Ad 1983 *Phys. Rev.* B **27** 6097
de Raedt H and Lagendijk Ad 1984 *Phys. Rev.* B **30** 1671

[8] Kornilovitch P E 1998 *Phys. Rev. Lett.* **81** 5382

[9] de Mello E and Ranninger J 1997 *Phys. Rev.* B **55** 14872
Capone M, Stephan W and Grilli M 1997 *Phys. Rev.* B **56** 4484
Alexandrov A S, Kabanov V V and Ray D K 1994 *Phys. Rev.* B **49** 9915
Wellein G and Fehske H 1997 *Phys. Rev.* B **56** 4513

[10] White S R 1993 *Phys. Rev.* B **48** 10345
Jeckelmann E and White S R 1998 *Phys. Rev.* B **57** 6376

[11] Ciuchi S, de Pasquale F, Fratini S and Feinberg D 1997 *Phys. Rev.* B **56** 4494

[12] Romero A H, Brown D W and Lindenberg K 1999 *Phys. Rev.* B **59** 13728

[13] Cataudella V, De Filippis G and Iadonisi G 1999 *Phys. Rev.* B **60** 15163

[14] Cataudella V, De Filippis G and Iadonisi G 2000 *Phys. Rev.* B **62** 1496

[15] Alexandrov A S 2000 *Phys. Rev.* B **61** 12315
Alexandrov A S and Sricheewin C 2000 *Europhys. Lett.* **51** 188

[16] Cappelluti E and Pietronero L 1996 *Europhys. Lett.* **36** 619

[17] Kulic M L 2000 *Phys. Rep.* **338** 1

[18] Fehske H, Loos J and Wellein G 2000 *Phys. Rev.* B **61** 8016

[19] Alexandrov A S and Yavidov B Ya 2003 *Preprint* cond-mat/0309061

[20] De Filippis G, Cataudella V, Marigliano Ramaglia V, Perroni C A and Bercioux D 2003 *Eur. Phys. J.* B **36** 65